

# Radiation Thermometry Toward the Triple Point of Water?

Jürgen Hartmann · Lutz Werner

Published online: 26 February 2008  
© Springer Science+Business Media, LLC 2008

**Abstract** The article describes and evaluates the possibility of using a high-temperature blackbody of accurately known thermodynamic temperature as a reference source for the determination of lower thermodynamic temperatures by spectral radiation thermometry. By applying various intermediate steps, this approach will allow spectral radiation thermometry to be used for the determination of the thermodynamic temperature of the triple point of water with a low uncertainty. The procedure for such an attempt is outlined, theoretical, and practical limits of the resulting uncertainty in thermodynamic temperature are given. The described experimental approach also provides a framework to calculate the uncertainties in determining the thermodynamic temperatures of the defining high-temperature fixed points of the International Temperature Scale of 1990 down to the triple point of water. The estimation of uncertainties is based on current and future values of the relevant contributing components. The uncertainty anticipated in determining the thermodynamic temperature of the triple point of water is 24 mK with current uncertainties and 1.9 mK in the future. Thus, the described approach yields uncertainties that are slightly higher, but comparable to, the tentative uncertainties of other methods—e.g., dielectric constant gas thermometry developed and applied within the framework of the new determination of the Boltzmann constant.

**Keywords** Absolute radiometry · Radiation thermometry · Spectral responsivity · Triple point of water

---

J. Hartmann (✉) · L. Werner  
Physikalisch-Technische Bundesanstalt, Braunschweig and Berlin, Abbestraße 2-12, 10587 Berlin,  
Germany  
e-mail: juergen.hartmann@ptb.de

## 1 Introduction

High-temperature measurements (above 961.78°C) carried out according to the prescriptions of the International Temperature Scale of 1990 (ITS-90) compare the spectral radiance of a blackbody of unknown temperature to that of a blackbody at the temperature of freezing silver, gold, or copper. It is a well-known consequence of relative radiation thermometry that the uncertainty of the reference temperature  $T_{\text{ref}}$  propagates to the uncertainty of the measured temperature  $T_{\text{meas}}$  via [1]

$$u(T_{\text{meas}}) = \left( \frac{T_{\text{meas}}}{T_{\text{ref}}} \right)^2 u(T_{\text{ref}}). \quad (1)$$

This fact limits the achievable uncertainty of the ITS-90 in the high-temperature range as the uncertainty of the silver, gold, or copper fixed-point temperature is propagated to the uncertainty of the ITS-90 temperature,  $T_{90}$ , of the unknown radiation source. Starting with the uncertainty of the thermodynamic temperature of freezing gold of 50 mK, the theoretical limit of the uncertainty in thermodynamic temperature near 3,250 K measured according to the ITS-90 is about 300 mK. It has been shown recently that high thermodynamic temperatures can be measured directly and independently of the ITS-90 by absolute radiometry, i.e., by using absolutely calibrated filter radiometers [2,3]. The spectral responsivity of such absolutely calibrated filter radiometers has to be traceable to a cryogenic radiometer, the primary detector standard [4]. Using absolute radiometry, high thermodynamic temperatures can be measured with uncertainties as low as those from, or even lower than those achieved with the ITS-90 methodology [2]. Equation 1 shows that by using a high-temperature blackbody as a reference source for radiation thermometry, the measurement of lower temperatures can be performed with uncertainties much lower than that of the reference source. Consequently, if the temperature of the high-temperature reference has been measured by absolute radiometry with an uncertainty lower than that achieved by the ITS-90, then the thermodynamic temperatures of fixed points at lower temperatures can be determined, in principle, with uncertainties lower than those of the ITS-90. The applicability of such an approach is described in this article.

According to the worldwide effort in re-determining the Boltzmann constant, a relative uncertainty in thermodynamic temperatures of about 1 to 2 ppm is envisaged in 2009 [5], i.e., about 250–500  $\mu\text{K}$  at the triple point of water (TPW). Using a high-temperature fixed point as a reference source for a radiation-thermometric determination of the TPW, an uncertainty of about 35–70 mK in the thermodynamic temperature of a blackbody at 3,250 K is necessary to achieve an uncertainty of 250–500  $\mu\text{K}$  at the TPW. The present article highlights the necessary requirements and the feasibility of such an approach, estimates the uncertainty that can currently be obtained, and anticipates what will be possible in the future.

## 2 Uncertainty of the Determination of the Thermodynamic Temperature of a High-Temperature Blackbody

The radiometric measurement of thermodynamic temperatures described in this article is based on the determination of the radiance emitted by a blackbody. The temperature  $T$  of the blackbody can then be calculated from the measured radiance  $L$  using Planck's law of radiation;

$$L_{\lambda,s}(\lambda, T) = \frac{2hc^2}{n^2\lambda^5} \frac{1}{\exp\left(\frac{hc}{kn\lambda T}\right) - 1} \quad (2)$$

where  $h$  is Planck's constant,  $k$  is Boltzmann's constant,  $c$  is the velocity of light,  $n$  is the index of refraction, and  $\lambda$  is the wavelength.

Filter radiometers are used to determine the radiance within a limited wavelength interval. The selection of the center wavelength of the filter radiometer is crucial because the uncertainty in temperature  $u_L(T)$  generated by the uncertainty  $u(L)$  of the measured radiance  $L$  strongly depends on the wavelength [6]

$$u_L(T) = \frac{\exp\left(\frac{hc}{kn\lambda T}\right) - 1}{\exp\left(\frac{hc}{kn\lambda T}\right)} T^2 \frac{kn}{hc} \lambda \frac{u(L)}{L}. \quad (3)$$

Equation 3 can be derived from Planck's law of radiation according to the *law of propagation of uncertainty* [7]. Equation 3 shows that the center wavelength of the filter radiometer should be chosen to be as short as possible in order to minimize the temperature uncertainty for a given uncertainty in radiance. However, the radiance of a blackbody decreases with decreasing wavelength on the short-wavelength side of its maximum. Consequently, the uncertainty of the radiance below a certain radiance level is dominated by the limited detectivity of the detector in the filter radiometer and increases with decreasing wavelength. The selection of the wavelength of the filter radiometer is therefore a compromise between the intention (i) to measure the blackbody's radiance with a low uncertainty and (ii) to achieve a low temperature uncertainty when the blackbody's temperature is calculated from its radiance. This compromise depends on the temperature of the blackbody and on the quality of the detectors available for the corresponding wavelength range.

In order to measure the spectral responsivity with the lowest uncertainties, detectors with the best characteristics have to be used. Quantum detectors have proven to be superior to thermal detectors with respect to stability, detectivity, and linearity. Within the quantum detectors, photovoltaic detectors are superior to photoconductive detectors [8]. Table 1 is a rough selection guide for detectors with respect to the range of blackbody temperatures. It lists relevant detector features, such as detectivity, noise equivalent power (NEP), and shunt resistance together with the estimated lower limit of the blackbody's temperature for which the detector is considered suitable.

Silicon photodiodes are best suited to the measurement of radiation emitted by high-temperature radiation sources, i.e., for temperatures above 850 K (see Table 1). For lower temperatures, detectors based on materials other than silicon have to be used.

**Table 1** Selection guide: typical data for the detectors best suited to the measurement of the respective temperature

| Detector material  | Si                    | InGaAs                | Extended InGaAs       | InSb                  |
|--|-----------------------|-----------------------|-----------------------|-----------------------|
| Peak wavelength (nm)   | 960                   | 1,600                 | 2,300                 | 5,000                 |
| Detectivity<br>( $\text{cm} \cdot \text{Hz}^{1/2} \cdot \text{W}^{-1}$ ) | $6 \times 10^{14}$    | $3 \times 10^{13}$    | $2 \times 10^{12}$    | $1.6 \times 10^{11}$  |
| NEP ( $\text{W} \cdot \text{Hz}^{-1/2}$ )                                | $1 \times 10^{-15}$   | $1 \times 10^{-14}$   | $1.8 \times 10^{-12}$ | $1.6 \times 10^{-12}$ |
| Detector size, diameter (mm)   | 3                     | 3                     | 3                     | 3                     |
| Max. responsivity ( $\text{A} \cdot \text{W}^{-1}$ )                     | 0.62                  | 1.2                   | 1.2                   | 2.5                   |
| Lowest measurable<br>fixed-point temperature (K)                         | 933                   | 692                   | 429                   | 273                   |
| Typical signal at lowest<br>measurable fixed-point<br>temperature (A)    | $1.3 \times 10^{-11}$ | $1.5 \times 10^{-10}$ | $2.0 \times 10^{-10}$ | $2.5 \times 10^{-9}$  |

InGaAs is a mixed-crystal semiconductor material for the fabrication of photodiodes with a spectral responsivity peaking in the near-infrared (NIR) region. Common photodiodes made from InGaAs have a maximum spectral responsivity around 1,600 nm and can be used for temperatures down to about 500 K. For even lower temperatures, NIR-extended InGaAs photodiodes can be applied that are made up of InGaAs with a higher InAs content. These photodiodes exhibit maximum spectral responsivity in the vicinity of 2,500 nm and enable the measurement of radiation temperatures down to about 270 K. Below 270 K, InAs and InSb photodiodes with a spectral responsivity maximum above 2,500 nm can be used.

The photocurrent  $I_{\text{photo}}$  of a filter radiometer when measuring the radiation of a blackbody can be calculated according to

$$I_{\text{photo}} = \int_0^\infty s_{\text{irr}}(\lambda) E_\lambda(\lambda, T) d\lambda = \varepsilon G \int_0^\infty s_{\text{irr}}(\lambda) L_{\lambda,s}(\lambda, T) d\lambda, \tag{4}$$

with  $G$  describing the geometry,  $s_{\text{irr}}(\lambda)$  represents the spectral irradiance responsivity of the filter radiometer,  $E_\lambda(\lambda, T)$  denotes the spectral irradiance at the position of the filter radiometer, and  $L_{\lambda,s}(\lambda, T)$  is the spectral radiance of the blackbody according to Planck’s law of radiation.  $\varepsilon$  is the emissivity of the blackbody,  $T$  is the temperature of the blackbody, and  $\lambda$  is the wavelength. Within the passband of narrow-band interference filter radiometers, the spectral variation of Planck’s law of radiation can be neglected for the purpose of the uncertainty calculation and Eq. 4 can be rewritten as follows [9]:

$$I_{\text{photo}} = \varepsilon G \int_0^\infty s_{\text{irr}}(\lambda) L_{\lambda,s}(\lambda, T) d\lambda \approx \varepsilon G L_{\lambda,s}(\lambda_c, T) \int_0^\infty s_{\text{irr}}(\lambda) d\lambda, \tag{5}$$

where  $\lambda_c$  is the center wavelength of the filter radiometer calculated according to

$$\lambda_c = \frac{\int_0^{\infty} \lambda s_{\text{irr}}(\lambda) d\lambda}{\int_0^{\infty} s_{\text{irr}}(\lambda) d\lambda}. \quad (6)$$

According to Eq. 5, three major uncertainty contributions have to be considered when measuring the thermodynamic temperature of a blackbody. They arise from (i) the absolute spectral responsivity of the filter radiometer, (ii) the geometry factor  $G$  of the measurement, including the emissivity of the blackbody, and (iii) the numerical calculation of the temperature using the measured photocurrent. In the following, these three components are considered separately. For each contribution, the current lowest uncertainties and the foreseen best future uncertainties are given.

## 2.1 Spectral Responsivity

Currently, the lowest uncertainties in the calibration of the spectral responsivity can be obtained in the visible spectral range using silicon photodiodes [10]. Table 2 summarizes the uncertainty components for the spectral responsivities at the shortest wavelength currently used with absolutely calibrated filter radiometers at the Physikalisch-Technische Bundesanstalt (PTB), i.e., 476 nm. As mentioned above, the center wavelength of the filter radiometer should be as short as possible to achieve the lowest uncertainties in temperature. The current limit of 476 nm is due to the lack of sufficiently narrowly spaced additional laser lines at lower wavelengths for the calibration of the transfer detector against the cryogenic radiometer [4, 10]. In the future, a frequency-doubled Ti:sapphire laser is intended to be used to calibrate the transfer detector, which is usually a trap detector, against the cryogenic radiometer down to 350 nm. This trap detector will then be used to calibrate the filter radiometers at 400 nm (and even 350 nm) center wavelengths with uncertainties as low as, or even lower than, those in the visible spectral range. The use of silicon photodiodes at UV wavelengths has been investigated thoroughly, and no additional uncertainties are expected for wavelengths above 300 nm [11]. The use of a monochromator grating with a line density increased by a factor of two would increase the wavelength accuracy by a factor of two. A larger input aperture of the trap detector and the filter radiometer enabled by larger silicon photodiodes will reduce the uncertainty due to diffraction effects and the aperture area by a factor of two also.

## 2.2 Geometry

The geometry of the experiment is shown in Fig. 1. The main features are the areas of the two precision apertures and the distance between them. They allow for the determination of the radiance of the blackbody in terms of the irradiance measured by the filter radiometer. Table 3 shows the current and future uncertainty contributions arising from the geometric data and the emissivity of the blackbody cavity.

**Table 2** Uncertainty of the absolute spectral irradiance responsivity of silicon-based filter radiometers in relative units of  $10^{-4}$

| Wavelength (nm)  | Current |       | Future |       |
|--|---------|-------|--------|-------|
|  | 476     | 3,000 | 476    | 350   |
| Temperature (°C)   | 3,000   | 3,000 | 3,000  | 3,000 |
| <i>Filter radiometer, abs. calibration</i>                     |         |       |        |       |
| Spectral responsivity of transfer detector                     | 1.6     | 0.5   | 0.8    | 1.0   |
| Nonlinearity correction of transfer detector                   | 0.2     | 0.2   | 0.2    | 0.2   |
| Aperture area of transfer detector                             | 0.8     | 0.8   | 0.8    | 0.8   |
| Diffraction correction   | 1.0     | 0.5   | 0.5    | 0.5   |
| Distance from exit slit  | 0.3     | 0.3   | 0.3    | 0.3   |
| Temperature coefficient of transfer detector                   | 0.1     | 0.1   | 0.1    | 0.1   |
| Temperature coefficient of filter radiometer                   | 0.5     | 0.5   | 0.5    | 0.5   |
| Homogeneity of spectral comparator beam                        | 0.2     | 0.2   | 0.2    | 0.2   |
| Stability of tungsten halogen lamp                             | 0.2     | 0.2   | 0.2    | 0.2   |
| Uncertainty of center wavelength (current, 8 pm; future, 4 pm) | 0.7     | 0.4   | 0.6    | 0.9   |
| Total filter radiometer abs. calibration                       | 2.3     | 1.3   | 1.5    | 1.8   |

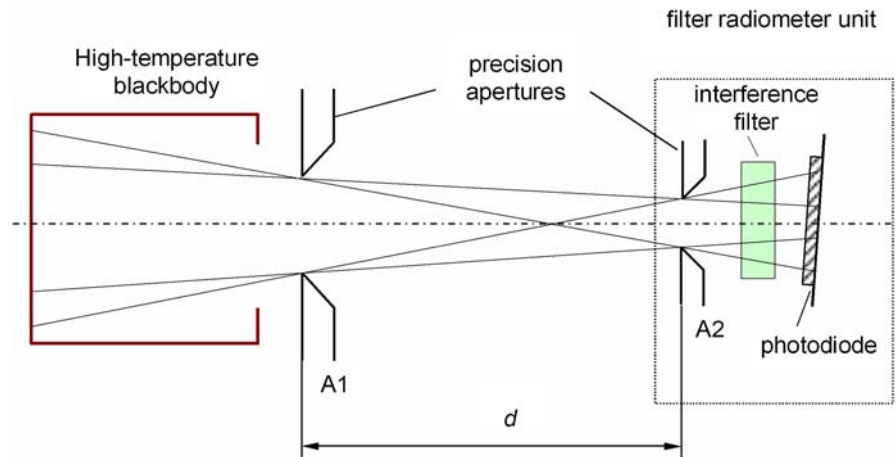


**Fig. 1** Geometry of absolute radiometry for measurement of the thermodynamic temperature of high-temperature blackbody

Only the uncertainty contributions due to the diffraction correction might be reduced in the future.

### 2.3 Measurement of the Photocurrent and Calculation of the Thermodynamic Temperature

The uncertainty of the photocurrent measurement is determined by the noise of the photocurrent, the calibration of the current-to-voltage converter, and the digital voltmeter.

**Table 3** Uncertainty contributions of the geometric data in relative units of  $10^{-4}$ 

|  | Current | Future |       |       |
|--|---------|--------|-------|-------|
|  |         | 476    | 400   | 350   |
| Wavelength (nm)  | 476     | 476    | 400   | 350   |
| Temperature ( $^{\circ}\text{C}$ )   | 3,000   | 3,000  | 3,000 | 3,000 |
| <i>Geometry (irradiance to radiance)</i>   |         |        |       |       |
| Area of BB aperture ( $20 \pm 0.0002$ mm)  | 0.2     | 0.2    | 0.2   | 0.2   |
| Thermal expansion of BB aperture   | 0.01    | 0.01   | 0.01  | 0.01  |
| Diffraction correction   | 1.5     | 1.0    | 1.0   | 1.0   |
| Aperture distance (current, $30 \mu\text{m}$ @ $1,000$ mm;<br>future, $15 \mu\text{m}$ ) | 0.6     | 0.3    | 0.3   | 0.3   |
| Emissivity of BB   | 1.0     | 1.0    | 1.0   | 1.0   |
| Total geometry   | 1.9     | 1.5    | 1.5   | 1.5   |

**Table 4** Contributions to the uncertainty of the photocurrent measurement and numerical integration in relative units of  $10^{-4}$ 

|  | Current | Future |       |       |
|--|---------|--------|-------|-------|
|  |         | 476    | 400   | 350   |
| Wavelength (nm)                                | 476     | 476    | 400   | 350   |
| Temperature ( $^{\circ}\text{C}$ )             | 3,000   | 3,000  | 3,000 | 3,000 |
| <i>Measurement of photocurrent</i>             |         |        |       |       |
| Photocurrent noise                             | 0.5     | 0.5    | 0.5   | 0.5   |
| Calibration of I/U-converter                   | 1.0     | 0.5    | 0.5   | 0.5   |
| Calibration of digital voltmeter               | 0.2     | 0.2    | 0.2   | 0.2   |
| Numerical calculation of photocurrent integral | 0.5     | 0.5    | 0.5   | 0.5   |
| Refractive index of air, $n$                   | 0.3     | 0.3    | 0.3   | 0.3   |
| Boltzmann constant, $k$ (CODATA 1998)          | 0.2     | 0.2    | 0.2   | 0.2   |
| Total photocurrent measurement                 | 1.3     | 1.0    | 1.0   | 1.0   |

Calculation of the thermodynamic temperature then requires numerical calculation of photocurrent integral 162 of Planck's law, and knowledge of the index of refraction in air. These sources of uncertainty together with the resulting combined uncertainty are given in Table 4. The calibration of the current-to-voltage converter is the only contribution that might be reduced significantly in the future by using specially adopted current-to-voltage converters.

#### 2.4 Overall Uncertainty of the Thermodynamic Temperature Measurement

The overall uncertainty of the radiance of the high-temperature blackbody is the square root of the sum of the aforementioned three components, and it is given in Table 5 for the current and future values of the contributing uncertainties. The uncertainty of the thermodynamic temperature of the blackbody can be calculated from the uncertainty of the spectral radiance measurement according to Eq. 3, and it is also given in Table 5.

The thermodynamic temperatures of a high-temperature blackbody at about 3,250 K can currently be measured with an uncertainty of 115 mK. Considering the aforemen-

**Table 5** Total relative uncertainty of the radiance measurement of the high-temperature blackbody in  $10^{-4}$  and the resulting uncertainty in the thermodynamic temperature in mK

|  | Current |       | Future |       |
|--|---------|-------|--------|-------|
|  |         |       |        |       |
| Wavelength (nm)                          | 476     | 476   | 400    | 350   |
| Temperature ( $^{\circ}\text{C}$ )       | 3,000   | 3,000 | 3,000  | 3,000 |
| Total filter radiometer abs. calibration | 2.3     | 1.3   | 1.5    | 1.8   |
| Total geometry                           | 1.9     | 1.5   | 1.5    | 1.5   |
| Total photocurrent measurement           | 1.3     | 1.0   | 1.0    | 1.0   |
| Total uncertainty                        | 3.2     | 2.2   | 2.3    | 2.5   |
| Temperature equivalent (mK)              | 115     | 77    | 69     | 64    |

tioned improvements, this uncertainty can be reduced to about 64 mK in the future. According to Eq. 1, a direct comparison of the high-temperature blackbody at 3,250 K with a blackbody at the TPW by an ideal radiation thermometer would result in an uncertainty in the temperature of the TPW of 850  $\mu\text{K}$  currently and 450  $\mu\text{K}$  in the future. However, direct comparison of a blackbody at 3,250 K and a blackbody at 273.16 K is not possible due to the wavelength dependence of Planck's law of radiation and the detectivity of the detectors. To account for this, several intermediate steps must be included, preferably using defining fixed points of the ITS-90 [12]. This procedure is outlined and described in the next section.

### 3 Radiation Thermometry to Reach the Triple Point of Water

The determination of the temperature of the TPW by radiation thermometry relative to a high-temperature blackbody is proposed through the successive use of different radiation thermometers. The measurements described below can either be performed using fixed-point blackbodies or heat-pipe blackbodies. The fixed-point blackbodies offer a direct link to the present ITS-90 and offer ultimate reproducibility though with the lack of geometrical flexibility, while the heat-pipe blackbodies offer wider flexibility regarding geometry and temperatures.

The lowest fixed-point temperature where silicon photodiodes are best suited for radiation thermometry is that of the aluminum fixed point at 660.323 $^{\circ}\text{C}$ , i.e., 933.473 K [12]. Using the high-temperature blackbody with its accurately measured thermodynamic temperature as the reference source, the temperatures of the gold, silver, and aluminum fixed-points can be determined by relative radiation thermometry. To evaluate the uncertainty contribution arising for these measurements, a high-accuracy radiation thermometer, e.g., the LP3 from IKE Stuttgart (Germany),<sup>1</sup> is used as a practical device. Knowledge of the relative spectral responsivity of the radiation thermometer,

<sup>1</sup> References to commercial products are provided for identification purposes only and constitute neither endorsement nor representation that the item identified is the best available for the stated purpose.



its non-linearity, its stability, and its size-of-source effect (SSE) are necessary for the uncertainty determination. As the radiation thermometer is only used as a transfer instrument, only the short-term stability is important. The short-term stability of the LP3 radiation thermometer is about  $1 \times 10^{-4}$  and can be reduced to  $0.5 \times 10^{-4}$  in the future. The spectral responsivity can be measured much like that of a filter radiometer. As only the relative spectral responsivity is needed, some components of Table 2 do not apply. Non-linearity of silicon photodiodes in the wavelength range from 600 to 900 nm has been found to be on the order of  $1 \times 10^{-4}$  in the photocurrent range from  $10^{-10}$  to  $10^{-3}$  A [4]. The SSE of the LP3 radiation thermometer has been determined in the literature several times and is of the order of some  $10^{-4}$ , but can be corrected. The remaining uncertainty is below  $0.5 \times 10^{-4}$ . The final uncertainty for the radiation thermometer is given in Table 6.

To calculate the uncertainty of the measured temperature  $T$  using radiation thermometry, the following equation is used [6]:

$$\begin{aligned}
 u(T) &= \sqrt{\left(\frac{\lambda T^2}{h_c/k} \frac{u(Q)}{Q}\right)^2 + \left(T \left(\frac{T}{T_{\text{ref}}} - 1\right) \frac{u(\lambda)}{\lambda}\right)^2 + \left(\left(\frac{T}{T_{\text{ref}}}\right)^2 u(T_{\text{ref}})\right)^2} \\
 &= \sqrt{u_Q^2(T) + u_\lambda^2(T) + u_{T_{\text{ref}}}^2(T)}. \quad (7)
 \end{aligned}$$

$Q$  denotes the ratio of the photocurrents measured by the radiation thermometer when viewing the high-temperature reference source at temperature  $T_{\text{ref}}$  and the source to be measured at temperature  $T$ . The parameter  $Q$  includes the uncertainty due to the relative spectral responsivity, the linearity, the photocurrent measurement, and the SSE. The resulting uncertainty in thermodynamic temperature of the aluminum, silver, and gold fixed points obtained by relative radiation thermometry with respect to the high-temperature blackbody is calculated according to Eq. 7 and is also given in Table 6. The current uncertainties in measuring the thermodynamic temperatures of the aluminum, silver, and gold fixed points are 15, 22, and 26 mK, respectively, and can be reduced to 8, 13, and 14 mK, respectively, in the future. These uncertainties are a factor of two to three lesser than the presently available uncertainties of the defined fixed-point temperatures of the ITS-90 with respect to thermodynamic temperature. If the spectral irradiance of the fixed point is directly measured with an absolutely calibrated filter radiometer, uncertainties can be achieved that are lower than those associated with the ITS-90 assignment of the fixed-point temperature, but significantly higher than the results obtained by relative radiation thermometry with respect to the high-temperature blackbody. The reason for this is that, on the one hand, a longer wavelength has to be used to measure the absolute irradiance of the low-temperature fixed points and, on the other hand, a small precision aperture has to be used to define the radiating area of the fixed-point blackbodies. The uncertainty that can be obtained by directly measuring the thermodynamic temperature of the aluminum fixed point with absolutely calibrated filter radiometers is 19 mK currently and should be 15 mK in the future.

Using the Al fixed point, the lowest fixed point measurable with silicon photodiode-based radiation thermometers, as a reference source for the measurement of the Sn fixed-point, an alternative radiation thermometer with a spectral responsivity maxi-

**Table 6** Current and future uncertainties of the temperatures of the silver, gold, or aluminum fixed points determined by relative radiation thermometry against a high-temperature blackbody

|                         |   | Current         |                  |                     | Future          |                   |                     |
|-------------------------|---|-----------------|------------------|---------------------|-----------------|-------------------|---------------------|
|                         | Fixed-point<br>Fixed-point<br>temperature (°C)          | Gold<br>1064.18 | Silver<br>961.78 | Aluminum<br>660.323 | Gold<br>1064.18 | Silver<br>961.323 | Aluminum<br>660.323 |
|                         | Wavelength of the<br>radiation thermometer<br>(nm)      | 650             | 650              | 900                 | 650             | 650               | 900                 |
|                         | Reference<br>temperature (°C)                           | 3,000           | 3,000            | 3,000               | 3,000           | 3,000             | 3,000               |
| $u_Q(T)$                | <i>Radiation thermometer (RT), relative calibration</i> |                 |                  |                     |                 |                   |                     |
|                         | Spectral responsivity<br>transfer detector              | 0.6             | 0.6              | 0.6                 | 0.3             | 0.3               | 0.3                 |
|                         | Nonlinearity<br>correction transfer<br>detector         | 0.2             | 0.2              | 0.2                 | 0.2             | 0.2               | 0.2                 |
|                         | Aperture area of<br>transfer detector                   | –               | –                | –                   | –               | –                 | –                   |
|                         | Diffraction correction<br>transfer detector             | –               | –                | –                   | –               | –                 | –                   |
|                         | Distance from exit slit<br>Temperature                  | –               | –                | –                   | –               | –                 | –                   |
|                         | Temperature<br>coefficient transfer<br>detector         | 0.1             | 0.1              | 0.1                 | 0.1             | 0.1               | 0.1                 |
|                         | Temperature<br>coefficient RT                           | 0.5             | 0.5              | 0.5                 | 0.3             | 0.3               | 0.3                 |
|                         | Homogeneity of<br>spectral comparator<br>beam           | 0.2             | 0.2              | 0.2                 | 0.2             | 0.2               | 0.2                 |
|                         | Stability of tungsten<br>halogen lamp                   | 0.2             | 0.2              | 0.2                 | 0.2             | 0.2               | 0.2                 |
|                         | <b>Relative spectral<br/>responsivity of RT</b>         | 0.9             | 0.9              | 0.9                 | 0.6             | 0.6               | 0.6                 |
|                         | <b>Non-linearity of RT</b>                              | 1.0             | 1.0              | 1.0                 | 0.5             | 0.5               | 0.5                 |
|                         | <b>Short-term stability<br/>of RT</b>                   | 1.0             | 1.0              | 1.0                 | 0.5             | 0.5               | 0.5                 |
|                         | <b>Size-of-source effect<br/>of RT</b>                  | 0.5             | 0.5              | 0.5                 | 0.5             | 0.5               | 0.5                 |
| $u_\lambda(T)$          | <b>Uncertainty in<br/>wavelength of RT<br/>(pm)</b>     | 8               | 8                | 8                   | 4               | 4                 | 4                   |
| $u_{T_{\text{ref}}}(T)$ | $u(T_{\text{ref}} = 3,000^\circ\text{C})$               | 115             | 115              | 115                 | 64              | 64                | 64                  |
| $u(T)$                  | <b>Temperature<br/>equivalent total<br/>(mK)</b>        | 26              | 22               | 15                  | 14              | 13                | 8                   |

**Table 7** Current and future uncertainties of the temperature of the Sn fixed point determined by relative radiation thermometry against the Al fixed point

|                         |   | Current | Future  |
|-------------------------|---|---------|---------|
|                         | Wavelength (nm)   | 1,550   | 1,550   |
|                         | Temperature (°C)  | 231.928 | 231.928 |
|                         | Reference temperature (°C)                                    | 660.323 | 660.323 |
| $u_Q(T)$                | <i>Radiation thermometer (RT), relative calibration</i>       |         |         |
|                         | Spectral responsivity transfer detector                       | 3.0     | 0.4     |
|                         | Nonlinearity correction transfer detector                     | 0.2     | 0.2     |
|                         | Aperture area of transfer detector                            | –       | –       |
|                         | Diffraction correction transfer detector                      | –       | –       |
|                         | Distance from exit slit                                       | –       | –       |
|                         | Temperature coefficient transfer detector                     | 0.5     | 0.1     |
|                         | Temperature coefficient radiation thermometer                 | 0.5     | 0.5     |
|                         | Homogeneity of spectral comparator beam                       | 0.2     | 0.2     |
|                         | Stability of tungsten halogen lamp                            | 0.2     | 0.2     |
|                         | <b>Relative spectral responsivity of RT</b>                   | 3.1     | 0.7     |
|                         | <b>Non-linearity of RT</b>                                    | 1.0     | 0.3     |
|                         | <b>Short-term stability of RT</b>                             | 1.0     | 0.3     |
|                         | <b>Size-of-source effect of RT</b>                            | 0.5     | 0.3     |
| $u_\lambda(T)$          | <b>Uncertainty in wavelength of RT (pm)</b>                   | 25      | 8       |
| $u_{T_{\text{ref}}}(T)$ | <b><math>u(T_{\text{ref}} = 660.323^\circ\text{C})</math></b> | 15      | 8       |
| $u(T)$                  | <b>Temperature equivalent total (mK)</b>                      | 11      | 4       |

mum further in the infrared region of the optical spectrum has to be used. According to Table 1, InGaAs photodiodes with a maximum spectral responsivity around 1,550 nm can be used in this temperature range. The detectivity of such InGaAs photodiodes is about a factor of 10 lower than the detectivity of silicon photodiodes and, therefore, requires a significantly longer integration time. The spectral responsivity of InGaAs detectors can be measured at PTB with uncertainties comparable to those of silicon photodiodes [13]. The relevant current and future uncertainties contributing to the total uncertainty of the measurement of the thermodynamic temperature of the Sn fixed point are shown in Table 7. The total measurement uncertainty of the thermodynamic temperature of the tin fixed point is currently 11 mK and can be reduced to 4 mK in the future.

For the last step from the Sn fixed-point temperature to the TPW, extended InGaAs photodiodes have to be used. As the temperature of the TPW is significantly below ambient temperature, the influence of the background radiation on the measured signals has to be considered or, preferably, prevented. To avoid undesired influence of the background radiation, the measurements of this last step will be performed using the low-background facility of PTB [14]. This facility offers an optical path that is cooled to liquid-nitrogen temperature, yielding negligible background radiation. The measurements at the low background facility are also performed under vacuum, preventing problems with absorption by water vapor and other gases. Using this low

background facility, the influences of background radiation and absorption on the measured signal of the TPW will be negligible. The uncertainty for the measurement of the spectral responsivity at wavelengths around 2,300 nm is currently considerably higher than in the spectral region below 1,700 nm and is estimated to be about 0.2%. Using tunable laser radiation in the future will reduce this uncertainty to the value currently obtainable in the spectral region below 1,700 nm. Table 8 shows the uncertainties that have to be taken into account when measuring the thermodynamic temperature of the TPW using extended InGaAs photodiodes. According to Table 8, the uncertainty in the thermodynamic temperature of the TPW obtainable with radiation thermometry is estimated to be 24 mK currently and can be lowered to 1.9 mK in the near future. Figure 2 schematically shows the four-step approach to measure the thermodynamic temperature of the TPW by radiometric methods with lowest uncertainties.

## 4 Discussion

Already today, radiation thermometry at PTB enables the thermodynamic temperature of the defining fixed points of the ITS-90 down to the aluminum fixed-point temperature to be determined with uncertainties lower than those associated with the ITS-90

**Table 8** Current and future uncertainties of the temperature of the TPW determined by relative radiation thermometry against the Sn fixed point

|                            | Current (estimated)   | Future  |
|----------------------------|---|---------|
| Wavelength (nm)            | 2,300   | 2,300   |
| Temperature (°C)           | 0.01  | 0.01    |
| Reference temperature (°C) | 231.928   | 231.928 |
| $u_Q(T)$                   | <i>Radiation thermometer (RT), relative calibration</i>       |         |
|                            | Relative spectral responsivity transfer detector              |         |
|                            | 20.0  | 0.4     |
|                            | Nonlinearity correction transfer detector                     |         |
|                            | 1   | 0.2     |
|                            | Aperture area of transfer detector                            |         |
|                            | –   | –       |
|                            | Diffraction correction transfer detector                      |         |
|                            | –   | –       |
|                            | Distance from exit slit                                       |         |
|                            | –   | –       |
|                            | Temperature coefficient transfer detector                     |         |
|                            | 1   | 0.1     |
|                            | Temperature coefficient radiation thermometer                 |         |
|                            | 0.5   | 0.3     |
|                            | Homogeneity of spectral comparator beam                       |         |
|                            | 0.2   | 0.2     |
|                            | Stability of tungsten halogen lamp                            |         |
|                            | 0.2   | 0.2     |
|                            | <b>Relative spectral responsivity of RT</b>                   | 20.1    |
|                            | <b>Non-linearity of RT</b>                                    | 1.0     |
|                            | <b>Short-term stability of RT</b>                             | 1.0     |
|                            | <b>Size-of-source effect of RT</b>                            | 1.0     |
| $u_\lambda(T)$             | <b>Uncertainty in wavelength of RT (pm)</b>                   | 25      |
| $u_{T_{\text{ref}}}(T)$    | <b><math>u(T_{\text{ref}} = 231.928^\circ\text{C})</math></b> | 11      |
| $u(T)$                     | <b>Temperature equivalent total (mK)</b>                      | 24.4    |
|                            |   | 1.9     |

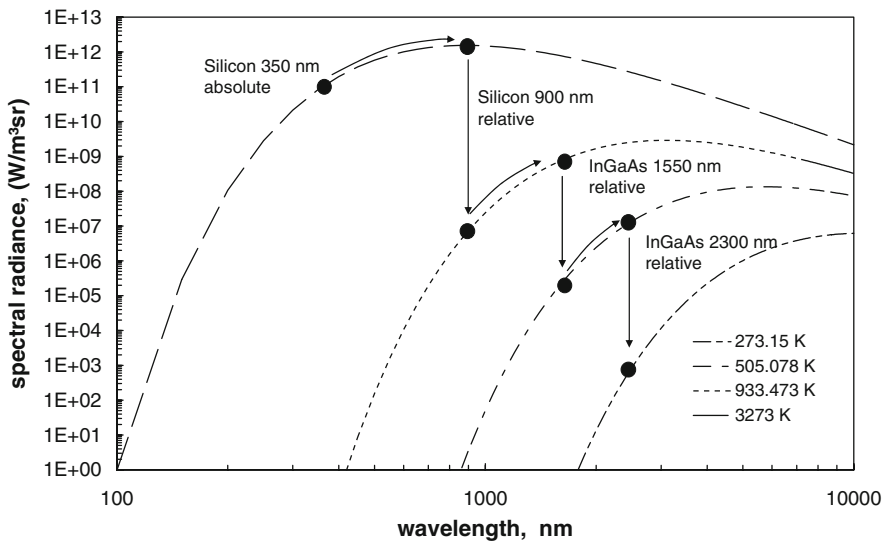


**Fig. 2** Schematic representation of the four-step approach to measure the thermodynamic temperature of the TPW with radiometric methods with lowest uncertainties. The challenge of the huge difference in the spectral radiance in the case of the TPW temperature measurement with respect to the tin point is addressed by using a wider bandwidth of about 250 nm and a longer integration time

assigned values. In the near future, even the thermodynamic temperatures of the zinc and tin fixed points will be measurable with uncertainties lower than those of the current ITS-90 values.

It has been shown that the uncertainty in the determination of the thermodynamic temperature of the TPW using radiation thermometry is currently about 24 mK and can be lowered to 1.9 mK in the near future. A purely hypothetical approach to measuring the thermodynamic temperature of the TPW using extended InGaAs photodiodes directly with respect to the Al fixed point or the HTBB at 3,250 K would result in uncertainties of 1.8 and 1.6 mK, respectively. However, such measurements do not seem realistic, as the ratio of the signals at the Al fixed point and at 3,250 K to those at the TPW are on the order of  $10^7$  and  $10^9$ , respectively.

The uncertainty of 1.9 mK achievable by radiation thermometry in the near future is slightly higher than, but comparable to, the target uncertainties of other absolute thermometric methods and show that radiation thermometry, in principle, allows measurements of the TPW temperature with sufficiently low uncertainty. If an effort to improve the spectral responsivity measurement is increased considerably, requiring, in particular, significant improvements in the performance of NIR photovoltaic detectors, the uncertainties can be significantly lowered, resulting in uncertainties of the thermodynamic temperature of the TPW less than 1 mK.

**Acknowledgments** Fruitful and continuing discussions with Berndt Gutschwager and Dieter Taubert are gratefully acknowledged.

## References

1. T. Quinn, *Temperature* (Academic Press Ltd., London, 1983)
2. K. Anhalt, J. Hartmann, D. Lowe, G. Machin, M. Sadli, Y. Yamada, *Metrologia* **43**, S78 (2006)
3. H.W. Yoon, *Metrologia* **43**, S22 (2006)
4. L. Werner, J. Fischer, U. Johannsen, J. Hartmann, *Metrologia* **37**, 279 (2000)
5. B. Fellmuth, Ch. Gaiser, J. Fischer, *Meas. Sci. Technol.* **17**, R145 (2006)
6. H.J. Jung, in *Proceedings of TEMPMEKO '96, 6th International Symposium on Temperature and Thermal Measurements in Industry and Science*, ed. by P. Marcarino (Levrotto and Bella, Torino, 1997), pp. 235–244
7. International Organization for Standardization, 1993 *Guide to the Expression of Uncertainty in Measurement* (ISO, Geneva, 1993)
8. See, e.g., *Technical Information SD-12*, Hamamatsu, www.hamatsu.de
9. D.R. Taubert, R. Friedrich, J. Hartmann, P. Sperfeld, J. Hollandt, in *Proceedings of TEMPMEKO 2004, 9th International Symposium on Temperature and Thermal Measurements in Industry and Science*, ed. by D. Zvizdić, L.G. Bermanec, T. Veliki, T. Stašić (FSB/LPM, Zagreb, Croatia, 2004), pp. 977–982
10. D.R. Taubert, R. Friedrich, J. Hartmann, J. Hollandt, *Metrologia* **40**, S35 (2003)
11. L. Werner, *Metrologia* **35**, 407 (1998)
12. H. Preston-Thomas, *Metrologia* **27**, 3 (1990)
13. N. Noulkow, R.D. Taubert, P. Meindl, J. Hollandt, in *Proceedings of TEMPMEKO 2007* (to be published in *Int. J. Thermophys.*)
14. C. Monte, B. Gutschwager, S.P. Morozova, J. Hollandt, in *Proceedings of TEMPMEKO 2007* (to be published in *Int. J. Thermophys.*)